TOMOGRAPHIC RECONSTRUCTION OF PROBABILITY DENSITY FUNCTIONS IN TURBULENT FLAMES

Pumyos Vallikul, Robert Goulard, Catherine Mavriplis,
The George Washington University, Washington DC 20052 USA
and
Marc R. Nyden,
National Institute of Standards and Technology, Gaithersburg, MD 20899 USA

ABSTRACT

Local probability density functions (PDF) of absorption coefficients within turbulent flames have been retrieved from their multi-angular absorption data of path-integrated probability density functions via a series of numerical techniques. First the Filter Back-Projection (FBP) technique has been used to reconstruct local moments within the flame then the moments are transformed to the local PDFs by using the singular value decomposition (SVD) technique. The FBP technique transforms the absorption data into the frequency domain where noisy components can be truncated while turbulent components are still preserved in the form of reconstructed moments. The reconstruction algorithm is tested by using both synthetic and experimental absorption data. Reconstruction from synthetic data allows the reconstruction algorithm to be evaluated independently of path measurement noise. On the other hand, reconstruction from experimental data demomstrates the capability of determining the local PDF analytically within the turbulent flame. Good reconstruction results are obtained from both cases and the reconstruction algorithm is justified.

INTRODUCTION

Electromagnetic and acoustic waves are widely used as nonintrusive diagnostics[1-5]. The interaction between waves and the material inside the volume of interest is in turn related to the thermodynamic properties of the medium (density, temperature, species concentration). There are two broad approaches to wave measurements: path and point measurements. Path measurements integrate the interactions taking place along a line between the source and the sensor. This measure is adequate for uniform samples, but it is not applicable in those cases where concentrations vary along the line of sight. This is not the case for point measurements: the interaction is limited to the small volume where the optical path from the source overlaps the optical path or scattered or fluorescent energy which is captured by the sensor. Therefore, point measurements have an unambiguous spatial simplicity, generally insensitive to non-homogeneity along the paths.

There are, however, a number of situations where the convergence of two paths is not possible (as in all emission measurements): the beam path is not unaffected outside the test volume; the physics of beam-matter interaction may be unfavorable in the application of interest (weak cross-section, quenching, etc.); or it is desirable to measure a property at many points in a region simultaneously. In such cases,

Intl. Interflam '96 Conf., 7th Proc. March 26-28, 1996, Cambridge, England. Franks, C.A., Grayson, S., Eds. Interscience Communications Ltd., London, England, 1996.

it may be necessary to revert to path techniques, with the concurrent need to eliminate the ambiguity of path averaged signals by analytical methods.

An optical absorption tomography method - a path measurement technique - has been used successfully in combustion diagnostics as an analytical method for reconstructing temperature and concentration profiles within laminar flames from their multi-angular absorption measurement data[6]. Recently, Sivathanu and Gore[7] proposed onion peeling tomography in conjunction with a discrete probability density function (DPF) method to infer the PDF of local extinction coefficients within turbulent flames from absorption measurements of PDFs of path-integrated transmittances. The reconstruction results appear reasonable, however they suffer from accumulation errors due to the peeling process.

In this paper, we propose to further develop Sivathanu and Gore's method by (1) introducing mathematical transform techniques to improve reconstruction results and by (2) directly calculating the PDF from the moments of the property field. There are two main advantages to mathematical transform techniques. First, they allow absorption data to be transformed into frequency domain where noisy components can be truncated. Second, they are easy to implement since they are explicit. The second part of the proposed method offers a way to preserve turbulent structure of the flow through the number of moments used in the method. The idea is to reconstruct the higher moments in addition to the first moment (the average value) of the property field. Once the moments are known, the problem then becomes the classical moment problem: given moments, find the density function. This work extends the capability of the tomographic method so that it can handle turbulent flame diagnostics in addition to the well-known application to laminar flame diagnostics.

A DENSITY FUNCTION OF TRANSMITTANCE AND ITS MOMENTS

In absorption measurements of turbulent flames[7], transmittance is defined discretely as a stochastic variable $\tau_{S,i}$ which represents all probable values of τ_S in an interval $\Delta\tau_S$ and the probability of occurrence of $\tau_{S,i}$ is measured as P_i. The discrete probability is related to the continuous PDF via P_i, $\tau_{S,i}$ and $\Delta\tau_S$ by

$$P_i = \int_{\tau_{S,i}-\Delta\tau_S/2}^{\tau_{S,i}+\Delta\tau_S/2} pdf(\tau_S)d\tau_S , \qquad [1]$$

where $pdf(\tau_S)$ is PDF of τ_S. It then follows that the n^{th} moment of τ_S can be calculated from the discrete probability by

$$M_{S,n} = \int \tau_S{}^n pdf(\tau_S)d\tau_S \equiv \sum_{i=1}^{N} \tau_{S,i}{}^n P_i \qquad [2]$$

where $M_{S,n}$ is the n^{th} moment of τ_S. Considering transmittance in a gas volume for a path length S consisting of two segments S1 and S2 with individual transmittances τ_{S1} and τ_{S2} , the total transmittance is

$$\tau_S = (\tau_{S1})(\tau_{S2}). \qquad [3]$$

Assume that the distributions of τ_{S1} and τ_{S2} are statistically independent, the variables τ_S, τ_{S1} and τ_{S2} can then be written respectively in terms of their moments as

$$M_{S,n} = (M_{S1,n})(M_{S2,n}). \quad [4]$$

Within each region S1 and S2, the local transmittance's measurements are made with an optical probe of a fixed path length Sm, giving the measured moments M_{m1} and M_{m2} respectively. Rewriting equation [4] in terms of the measured moments, we have

$$M_{S,n} = (M_{m1,n})^{S1/Sm}(M_{m2,n})^{S2/Sm} \quad [5]$$

Equation [5] shows that we can calculate explicitly the path-integrated moments from their local measurements of PDF along the path. Once $M_{S,n}$ are known, the P_i for all $\tau_{S,i}$ can be solved, using the linear equation [2], resulting in the path-integrated PDF.

The problem is reversed in absorption tomography. The path-integrated data are known and the local moments are required. The FBP algorithm[8] will be used for reconstructing the local moments from their multi-angular absorption measurement data. Other mathematical transformation techniques such as Hilbert transforms[9] or Wavelet transforms[10] can also be used to reconstruct the local moments. The formulae obtained by those mathematical transformation techniques are still explicit.

THE FBP ALGORITHM

The projection

A projection of a property field f(x,y) is a mapping of a two-dimensional function into a one-dimensional function obtained by integrating the function in a particular direction. It is generally convenient to refer the function to the (r,s) coordinate system, rotated from the (x,y) coordinate axis by an angle of θ. The projection of f(r,s) is

$$p_\theta(r) = \int_{-\infty}^{\infty} f(r,s)ds, \quad [6]$$

where $r = x\cos(\theta)+y\sin(\theta)$ and $s = -x\sin(\theta)+y\cos(\theta)$.

The Projection-slice theorem

Basically, the theorem states that the one-dimensional Fourier transform of a projection is a "slice" through the two-dimensional Fourier transform of the original function. Let $P_\theta(R)$ and F(R,S) be the Fourier transforms of $p_\theta(r)$ and f(r,s) then

$$P_\theta(R) = F(R,S)|_{S=0}, \quad [7]$$

where $R = X\cos(\theta)+Y\sin(\theta)$ and $S = -X\sin(\theta)+Y\cos(\theta)$.

The reconstruction formula

It follows from the Projection-slice theorem that if an infinite number of Fourier slices are taken from the corresponding infinite number of projections, F(X,Y) would be known at all points in the (X,Y) plane. Knowing F(X,Y), the property field f(x,y) can be recovered by using the inverse Fourier transform:

$$f(x,y) = \frac{1}{4\pi^2}\int_0^{\pi}\int_{-\infty}^{\infty} P_\theta(R)|R|e^{iR[x\cos(\theta)+y\sin(\theta)]}dRd\theta. \qquad [8]$$

Since |R| does not converge, R should be limited to some value $|R| \le \Omega$, and $P_\theta(R)$ should be small for $|R| > \Omega$. Let us introduce

$$H(R) = b(R)|R|, \qquad [9]$$

where $b(R) = 1$ if $|R| \le \Omega$, and $b(R) = 0$ for $|R| > \Omega$. Replacing |R| by H(R) and using the convolution theorem, equation [8] becomes

$$f(x,y) = \frac{1}{2\pi}\int_0^{\pi}\int_{-\infty}^{\infty} p_\theta(\tau)h(r-\tau)d\tau d\theta, \qquad [10]$$

where h(r) is the inverse Fourier transform of H(R). The above formula is called the Filter Back-Projection since the projection function $p_\theta(r)$ has been filtered by the ramp filter h(r), and the filtered projection functions for all angles are then back-projected onto the (x,y) coordinate system. Equation [10] is approximated by a discrete form as

$$f(x,y) = \frac{a}{2N}\sum_{j=1}^{N}\sum_{k=1}^{M} p_{\theta_j}(r_k)h(x\cos(\theta_j)+y\sin(\theta_j)-r_k), \qquad [11]$$

where N is the number of discrete angles, M is the number of discrete points along r, a is the length of the interval along r, $\theta_j = j\pi/N$ and $r_k = ka$. The filtered projection functions at the point $r = x\cos(\theta_j)+y\sin(\theta_j)$ may not correspond to the discrete points r_k: in those cases we interpolate the values between the known discrete points.

APPLICATION OF FBP TO RECONSTRUCTING PDFS OF LOCAL TRANSMITTANCE

The assumption of spatially independent PDFs of local transmittace discussed earlier allows us to define local moment of transmittance based on unit path-length as an intensive property. The path-integrated moment can be written in the two-dimensional (r,s) coordinate as

$$-\ln[M_\theta(r)] = -\int_{-\infty}^{\infty} \ln[m(r,s)]ds, \qquad [12]$$

where the local moment is referred to by a point in two-dimensional space instead of a segment in one-dimensional space, integration has been used instead of summation (this can be done since the local moment is an intensive property), and the integration path length has been changed to infinity since outside the region of interest all local moments are unity and the log of unity is zero. The resulting

path-integrated moment M is along the line perpendicular to the theta-line with a distance r from the origin. Since the moment equation [12] can be applied for all orders of moments, we drop the subscript n. The minus signs are introduced in order to get positive quantities for both sides of the equation. Although the notations are different, the physical representation of the path-integrated moments in equations [5] and [12] are similar. It follows from equations [6] and [12] that

$$f(r,s) = -\ln[m(r,s)], \qquad [13]$$

and

$$p_\theta(r) = -\ln[M_\theta(r)]. \qquad [14]$$

In the reconstruction problem, the path-integrated moments (the projections) are given and the local moments are unknowns. Equation [11] is used to reconstruct the local moments, which are then used in equation [2]. The resulting linear system is solved using the SVD[11] technique. The solution to the linear equation gives the discrete probabilities that can be used to interpret the PDF of the local transmittances which is in turn related to the PDF of absorption coefficient[7].

SVD METHOD FOR SOLVING AN OVERDETERMINED SYSTEM

Since the resolution of $\Delta\tau$ in equation [1] is limited, equation [2] becomes an overdetermined system of linear equations with M calculated moments and N unknown discrete probabilities. Equation [2] will be solved by the SVD method[11]. Rewrite equation [2] into the form

$$Ax = b, \qquad [15]$$

where A is the M x N transformation matrix, x is a vector representing all P_i and b is a vector representing all reconstructed moments at a particular point in (x,y) coordinate, $m(x_o,y_o)$. Any M by N matrix A of rank r can be factored[12] into

$$A = U\Sigma V^T, \qquad [16]$$

where U is an M x M orthogonal matrix, Σ is a M x N diagonal matrix of the form

$$\Sigma = \begin{bmatrix} S_{11} & 0 \\ 0 & 0 \end{bmatrix}_{M\times N} \qquad [17]$$

where S_{11} is a r x r diagonal matrix. The diagonal entries of S_{11} are strictly positive and can be arranged to be nonincreasing, $\sigma_1 > \sigma_2 > \ldots > \sigma_r > 0$. They are the singular values of A. V is an N x N orthogonal matrix.

The columns of U and V give orthonormal bases for all four fundamental subspaces[4] of A: the first r columns of U represent the column space; the last M-r columns of U the left nullspace; the first r columns of V the row space and the last N-r columns of V the nullspace of A[13]. The SVD method gives the unique solution that minimizes ||Ax-b|| by setting the left nullspace to zero. Golub's algorithm for calculating the SVD in double precision is used in this work. Basic aspects of the SVD and the details of Golub's algorithm are discussed by Wilkinson[14].

RECONSTRUCTION FROM SYNTHETIC PROJECTIONS

The proposed reconstruction method is used to reconstruct the PDF of local transmittance of a Propylene/Air diffusion flame. Local absorption measurements of the local PDFs within the flame are carried out by Sivathanu and Gore in their earlier work. The diameter of the burner used is 50 mm and the burner operates at the Reynolds number 750 based on fuel properties at the burner exit. A purge optical probe with a 10 mm path length was used to obtain the local PDFs from the absorption measurements. All local measurements are conducted in a plane (assumed circular) at a particular height above the burner (at x/d = 6. 7 where x is the distance from the burner surface and d is the burner diameter). The plane is divided into 11 rings and a central core where the local PDFs for the individual region are measured.

The measured local PDFs are used as test PDFs. in this paper. The projections are generated synthetically using the test PDFs and the moment method. Figure 1 shows the first moment of the test PDFs as a function of radial position and Figure 2 shows the corresponding projection function. To verify the path-integrated PDFs, the projection results are compared with the results calculated by using the DPF method introduced by Sivathanu and Gore. Figure 3 and Figure 4 show a comparision of PDFs of the path-integrated transmittances that passed through 9 and 11 outer-rings respectively calculated by the two methods. The results are in good agreement. The advantage of synthesizing the path integrated data is that the algorithm for reconstructing the PDF can be evaluated independent of path measurement noise.

All the reconstructed moments (the output from the FBP algorithm) at the center of the flame are gathered as components of the vector b plotting $\log_{10}(|U^T b|_n)$ and $\log_{10}(\sigma_n)$ values vs. the element number, we see in Figure 5 that the reconstructed moments give a consistent system of linear equations since the values of $|U^T b|$ vanished before the singular values. When the reconstruction is from synthetic projection data we can judge the quality of the reconstruction by comparing it to the test PDF. Figure 6 shows the reconstruction result compared with the test PDF at the center of the flame.

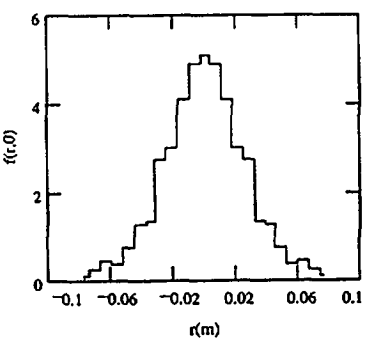

Figure 1 First moment of test-PDF (Propylene/ Air diffusion flame, Re=750, at x/d=6.7) as a function of radius

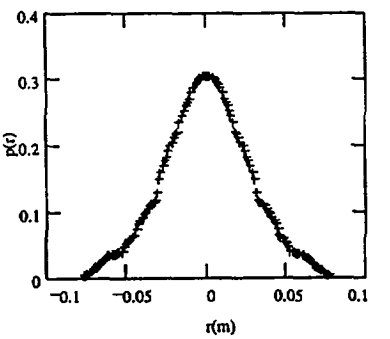

Figure 2 Synthetic Projection function of the first moment in Figure1

Reconstructing moments by using FBP algorithm with synthetic projections (180 projection angles and 128 line of sights for each angle) gives negligible error. The PDF solution from SVD method does not

match exactly to the test PDF since the number of the reconstructed moments is finite. However the discrepancy becomes negligible when more moments are included. The number of singular values used also affects the accuracy of the solution. The PDF solution shown in Figure 6, used 250 moments (0^{th}-299^{th} moment) and 18 singular values (σ_{min}~10^{-5}, and $\sigma_{max}/\sigma_{min}$ ~10^{5}). Deviation of total probability is less that 10^{-3} % from unity.

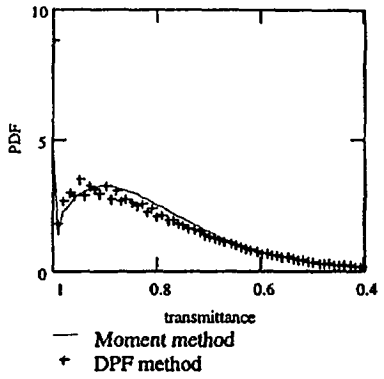

Figure 3 Comparision of moment-method calculated and discrete PDFs of path-integrated transmittance (passed through 9 outer-rings)

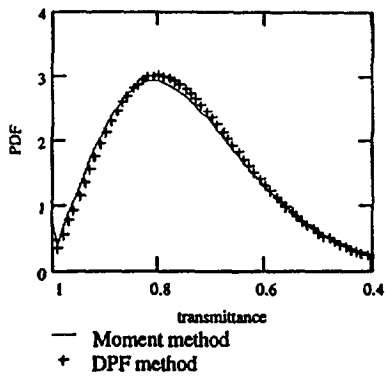

Figure 4 Comparision of moment-method calculated and discrete PDFs of path-integrated transmittance (passed through 11 outer-rings)

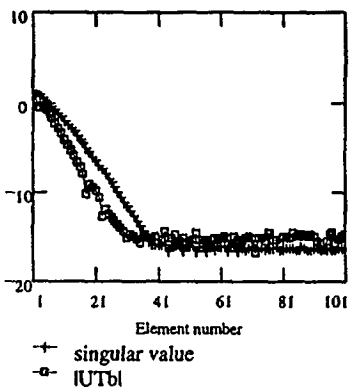

Figure 5 Singular value decomposition values: $\log_{10}(|U^{T}b|_n)$ and $\log_{10}(\sigma_n)$ from synthetic projection of Propylene/Air flame at center of flame

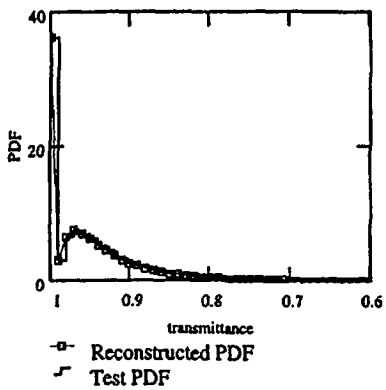

Figure 6 Reconstructed (from synthetic projection) and test PDFs at the center of Propylene/Air flame

RECONSTRUCTION FROM EXPERIMENTAL PROJECTIONS

A local PDF has been reconstructed from its measured projection and the reconstruction result has been compared with a measured PDF performed locally with a combustion flame. The flame is

Ethylene/Air turbulent jet flame with a 6 mm outlet-diameter and 9200 exit Reynolds number. The local measurement is at the center of a cross section (x/d = 30 above the burner) of the flame. It is shown in Figure 7 that the reconstructed moments do not give a consistent system of equations for all singular values since some of the singular values vanish before the components of $|U^T b|$. This implies that the vector of calculated moments is a linear combination of both the column space and the left nullspace of the transformation matrix A. To get the least squares solution, all singular values that are greater than the $|U^T b|$ have been used. In addition, the number of singular values used has to ensure a total probability closest to unity. The PDF solution shown in Figure 8, used 8 singular values ($\sigma_{min} \sim 10^{-1}$, and $\sigma_{max}/\sigma_{min} \sim 10^{2}$). Deviation of total probability is less than 7% from unity.

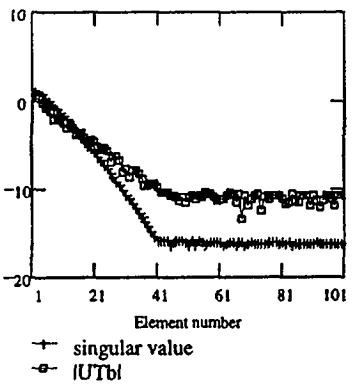

Figure 7 Singular value decomposition values: $\log_{10}(|U^T b|_n)$ and $\log_{10}(\sigma_n)$ from measured projection of Ethylene/Air flame at center of flame

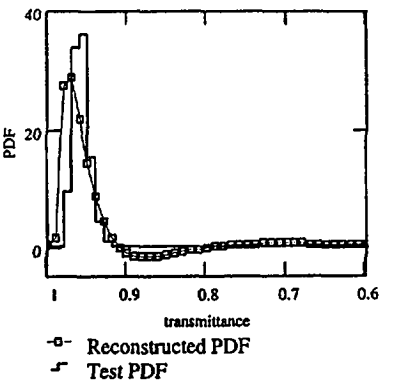

Figure 8 Reconstructed (from measured projection) and test PDFs at the center of Ethylene/Air flame

CONCLUSIONS AND FUTURE DIRECTIONS FOR RESEARCH

The synthetic data reconstruction result shows good agreement thereby validating the proposed method. Limited experimental data cause errors in both the FBP and the SVD calculation steps resulting in deviation of the reconstructed PDF from the measured PDF within the Ethylene/Air flame. However results are fairly good. Limited samples in projection cause aliasing effects in the FBP while limited floating point precision of both the measured data and the higher order moment calculations result in oscillations of the SVD-solution about the measured PDF. These are unfortunate errors that always appear in practice, but, these not withstanding, the assumption of spatially independent PDFs and the overall reconstruction algorithm are justified by our results. To reduce calculation cost, local tomography via wavelets transform and the maximum entropy method for predicting PDF from its limited moments are being investigated.

ACKNOWLEDGEMENT

Absorption measurement data used in this paper were supplied by Dr. Yudaya R. Sivathanu, School of Mechanical Engineering, Purdue University, during his stay in fall 1994 at National Institute of Standards and Technology (NIST), Gaithersburg, MD 20899 USA. Dr. Sivathanu's valuable

discussions are very much appreciated. We are also grateful to Bert W. Rust, Mathematician at NIST, for his suggestions and discussions on the SVD technique.

REFERENCE LIST

[1]Patel, D.K.N. "Laser Detection of Pollution." Science 202 (1979) : 157-173.

[2]Swindell, W. and Barrett, H.H. "Computerized Tomography: Taking Sectional X-Rays." Physics Today (1977) : 34-41.

[3]Hildebrand, B.P. and Brenden, B.P. An Introduction to Acoustical Holography. NewYork : Plenum Press, 1972.

[4]Vest, C.M. Holographic Interferometry. NewYork, New York : John Wiley and Sons, 1979.

[5]Goulard, R. (Ed.) Combustion Measurements. New York, New York : Academic Press, 1976.

[6]Chen, F.P. and Goulard, R. "Retrieval of Arbitrary Concentration and Temperature Fields by Multi-angular Scanning Techniques." JQSRT, Vol 16 (1976) : 819-827.

[7]Sivathanu, Y.R. and Gore, J.P. "A Tomographic Method for The Reconstruction of Local Probability Density Functions." JQSRT, Vol. 50, No.5 (1993) : 483-492.

[8]Shepp, L.A. and Logan B.F. "The Fourier Reconstruction of A Head Section." IEEE Transactions on Nuclear Science, Vol. NS-21 (1974) : 21-40.

[9]Herman, G.T. Image Reconstruction from Projections. Academic Press, 1980.

[10]Holschneider, M. "Inverse Radon Transforms Through Inverse Wavelet Transform." Inverse Problems, Vol 7 (1991) : 853-861.

[11]Golub, G.H. and Reinsch, C. "Singular Value Decomposition and Least Squares Solutions." Num. Math., Vol 14 (1970) : 403-420.

[12]Lawson, C.L. and Hanson, R.J. Solving Least Squares Problems. Prentice-Hall, Inc., 1974.

[13]Strang, G. Linear Algebra and Its Applications : 3rd edition. Harcourt Brance Jovanovich, Publishers, 1988.

[14]Wilkinson, J.H. "Singular-Value Decomposition-Basic Aspects." Numerical Software-Needs and Availability, Edited by D. Jacobs, Academic Press, 1978.